NANO LETTERS

xxxx
Vol. 0, No. 0
A−E

Fabrication of a 34 × 34 Crossbar Structure at 50 nm Half-pitch by UV-based Nanoimprint Lithography

G. Y. Jung,[†] S. Ganapathiappan,[†] Douglas A. A. Ohlberg,[†] Deirdre L. Olynick,[‡] Y. Chen,[†,||] William M. Tong,[†,§] and R. Stanley Williams*,[†]

Hewlett-Packard Laboratories, 1501 Page Mill Road, Palo Alto, California, 94304, Lawrence Berkeley National Laboratory, 1 Cyclotron Road, MS 02-400, Berkeley, California, 94720, and Technology Development Operations, Inkjet Technology Platform, Hewlett-Packard Company, 1000 Circle Boulevard, Corvallis, Oregon, 97330

Received April 5, 2004; Revised Manuscript Received May 13, 2004

ABSTRACT

We have developed a single-layer UV-nanoimprint process, which was utilized to fabricate 34 × 34 crossbar circuits with a half-pitch of 50 nm (equivalent to a bit density of 10 Gbit/cm^2). This process contains two innovative ideas to overcome challenges in the nanoimprint at shrinking dimensions. First, our new liquid resist formulation allowed us to minimize the residual resist layer thickness after curing and requires the relatively low imprint pressure of 20 psi. Second, by engineering the surface energy of the substrate we also eliminated the problem of trapped air during contact with the mold such that it spreads the resist and expels trapped air uniformly. Our overall process required fewer processing steps than any bilayer process and yielded high quality results at 50 nm half-pitch.

Optical lithography has been used to pattern semiconductor circuits for over three decades. However, as the feature sizes shrink to a small fraction of the wavelength of the light used, new challenges are emerging to drive the cost up dramatically. Hot embossing and its descendant nanoimprinting[1] have shown promise as new disruptive technologies to displace photolithography in patterning electronic circuits. These methods are attractive because of their promised high throughput with easy operation at a low cost. Such direct imprint techniques are already used to pattern "trailing-edge" products. However, with recent advances, the capability of imprinting has dramatically improved and begun to challenge that of cutting-edge optical lithography. It has now been incorporated into the 2003 version of the International Technology Road map for Semiconductors (http://public-.itrs.net/) for 32 nm half-pitch manufacturing (in 2013). Our demonstration of 50 nm half-pitch crossbar circuits is a significant milestone for the technique.

We have previously reported the fabrication of an 8 × 8 crossbar structure with 40 nm line width and 65 nm half-pitch by a thermal nanoimprint method.[2] Although our thermal nanoimprint process enabled us to achieve such small feature sizes, its inherent shortcomings became significant as our target feature size continued to shrink. One such shortcoming is the high imprint pressure: while our thermal process reduced the imprint pressure to 500 psi (14.7 psi = 1 atm) compared to that for the PMMA process (up to 2000 psi), this pressure was still high enough to be detrimental to the mold, which became less structurally robust as the feature size shrank. Another is thermal expansion mismatch between the substrate and the mold. It amplifies the difficulty in layer-to-layer alignment, which will be important in fabrication of future generations of devices. Our thermal nanoimprint process required the temperature to be ramped from room temperature to 70 °C. This change in temperature would destroy any submicrometer alignment between the mold and the substrate.

Alternative nanoimprint processes that utilize UV cured resists promised to resolve the aforementioned issues. The Willson group[3] pioneered the bilayer Step and Flash Imprint Lithography (S−FIL) process, which employed nanoimprinting to pattern the top layer that subsequently served as an etch stop to pattern the bottom layer. While this approach resolved the thermally related issues, it is by no means perfect. For example, a thick residual resist layer was left in the trenches after curing.[4] Its removal required an RIE step, which also tended to enlarge the desired feature size[5,6]

* Corresponding author: E-mail: stan.williams@hp.com, Phone: (+1)-650-857-6586, Fax:(+1)650-236-9885.
[†] Hewlett-Packard Laboratories.
[‡] Lawrence Berkeley National Laboratory.
[§] Technology Development Operations, HP.
[||] Present address: Department of Mechanical and Aerospace Engineering, UCLA, Los Angeles, California, 90024.

10.1021/nl049487q CCC: $27.50
Published on Web 00/00/0000

Table 1. Components of the Liquid Resist: Their Functions and Drawbacks

component	proportion (wt %)	function	drawback
benzyl methacrylate	67	active ingredient that polymerizes to form rigid structure	strong adhesion to the mold
tri-methylsiloxy silane	10	release agent to improve mold detachment	high viscosity impedes mold wetting/filling
poly(dimethyl) silane	20	lowers the overall viscosity of resist and improves the filling and wetting of the mold	does not polymerize; weakens the structure of cured resist
Irgacure 184	3	photoinitiator required for polymerization	

(known as "CD loss") and caused the fine features to collapse. In this paper, we describe an alternative single-layer process carried out in a new nanoimprinter with UV exposure capability (to be described in a future publication) and the use of this process to fabricate integrated nanoscale crossbar circuits.

Several issues were considered in formulating our new single-layer UV-curable resist for fabricating our crossbar circuit. Low viscosity was desired for easy flow through the empty channels between the mold and the substrate to yield a uniform film over the entire imprint area. It would also allow any resist trapped underneath the mold pattern to be extruded at a lower imprint pressure. While it is very important to have no residue under the trenches after imprinting, the cured resist must both adhere to the substrate and release from the mold without destroying the imprinted patterns. There is also a tradeoff between viscosity and the rate of polymerization. These are contradictory requirements that are difficult to satisfy simultaneously. Over 100 experimental trials were performed to optimize the formulation of this resist. Table 1 lists the optimum composition of resist with the functions and the disadvantages of each component. The main ingredient of the resist was benzyl methacrylate monomer (Aldrich). Irgacure 184 (absorption peak: 280 nm − 320 nm, Ciba) was used as the UV-sensitive free radical generator. (3-Acrylopropyl)tris(tri-methylsiloxy)silane (Gelest) served to lower the surface energy to allow for easy mold release. Poly(dimethylsiloxane) (viscosity: 1.0 cSt, Aldrich) was used primarily as the viscosity modifier, although its siloxane backbone also lowers the surface energy of the cured resist to facilitate mold release. It is important to note that the ideal proportions of the resist components depend strongly on factors such as pattern density on the mold, feature size, and feature-size distribution, and therefore need to be re-optimized for each application.

The mold was patterned by e-beam lithography at Lawrence Berkeley National Laboratory in a process that has been described previously.[7] Prior to first use, it was coated with a monolayer of organosilane molecules as a release agent in order to avoid adhesion of the cured resist to the mold. We employed a new method of vapor application for the release layer, the details of which will be in a forthcoming report.

Whereas the ability for the resist to be released by the mold after UV exposure is one of the critical requirements for nanoimprinting, the hydrophobic "release layer" applied onto the mold to prevent resist adhesion has two significant side effects. First, it prevents the liquid resist from penetrating into the pattern channels. Second, it impedes the uniform spreading of the resist during imprinting, since the resist has a tendency to bead up on the hydrophobic mold surface. Both these side effects lead to trapped air, which is detrimental to the fidelity of nanoimprinted patterns. At smaller feature sizes, expelling this trapped air during imprinting becomes even more difficult because of the increase in surface-to-volume ratio inside the mold grooves. Without modification to the process, the benefit of easy release would be nullified by the adverse effect of causing trapped air during mold−substrate contact.

Our solution to counterbalance this "negative-capillary action" on the mold was to raise the surface energy of the *substrate* to help spread the resist. When a substrate that had been made hydrophilic makes contact with the mold, the liquid resist, which had formed a bead on the hydrophobic mold surface, is forced by the high surface energy substrate to spread out, uniformly pushing out the air inside the nanosize channels and all hollow spaces of the mold (Figure 1). It is important to drop the liquid resist onto the clean Si mold and not onto the substrate. Otherwise, the resist spreads on the hydrophilic substrate surface before contact and makes it very difficult for any trapped air to escape after contact. The substrates were made of borofloat glass (for its transparency to UV light) with a thickness of 0.7 mm and polished to a low surface roughness of 0.4 nm rms. Our best results came from substrates that had been pretreated with a water-vapor plasma generated by a plasma source (Exi) for 10 min (p_{H_2O} = 0.7 Torr, power = 10 W). Still photos in Figure 2 show the resist-spreading process. The interference fringes present immediately after contact between the mold and the substrate (Figure 2a) showed nonuniform liquid resist thickness, but they spread out with time (Figure 2b) and disappeared after 30 min (Figure 2c), indicating a very uniform film over the entire contact area. The time needed for the fringes to disappear varied with the amount and the viscosity of the liquid resist dispensed. After complete spreading, the mold and substrate were adhered together so well that they could not be moved even with a strong lateral force. This was another indication of a uniform film with few trapped air bubbles.

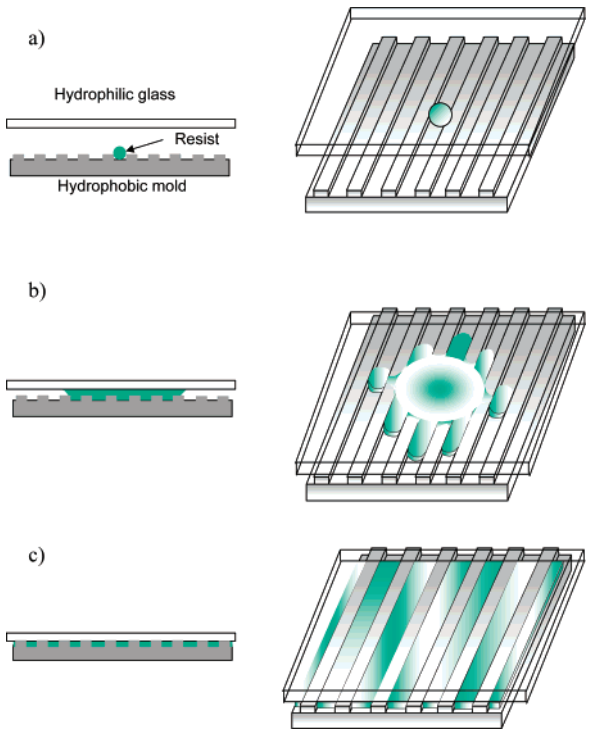

Figure 1. Our surface energy engineering scheme to promote the uniform spread of the resist. (a) The resist is applied to the hydrophobic mold and forms a bead. (b) Contact with the hydrophilic glass substrate causes the resist bead to spread. (c) Air is uniformly pushed out upon complete contact between the mold and the substrate.

The overall procedure used to make the crossbar circuit was similar to that for our thermal process,[2,7,8] in which a monolayer of switching material was sandwiched between crossed metal wires fabricated by a lift-off process. The key difference is that in this work we used a UV-curing process rather than the thermal-curing process. Because the contact between the mode and substrate surfaces after contact was not perfectly conformal, a residual liquid layer was trapped between them. This residual layer was squeezed out during the first step of the imprinting process, when a pressure of 20 psi was applied without irradiation for 10 min. Then the UV light from a mercury lamp source (280−320 nm) at an intensity of 7 W/cm^2 was turned on for 15 min to freeze in the pattern while the pressure was maintained. After this, the sample was removed from the nanoimprinter and the mold was detached from the substrate by hand. SEM cross-sections of imprinted areas revealed no obvious residual layer at the bottom of the imprinted trenches.

The thickness of the resist in the unpatterned regions was 60 ± 9 nm 3σ, as calculated from the profiles of 54 unpatterned regions between dies that had been scratched by a razor blade. The uniformity was reasonably high compared to bilayer processes, despite the presence of features of diverse sizes from sub-100 nm nanowires to large 100 μm-scale contact pads. The average thickness in the unpatterned region was less than that in the patterned nanowire regions (∼65 nm) or the relief height of the mold (∼70 nm), because the lack of structural support in the unpatterned region rendered the mold susceptible to bending under imprint pressure. We performed an oxygen RIE for 10 s at a power of 50 W and a pressure of 20 mTorr to descum any latent residual layer not observable by SEM.

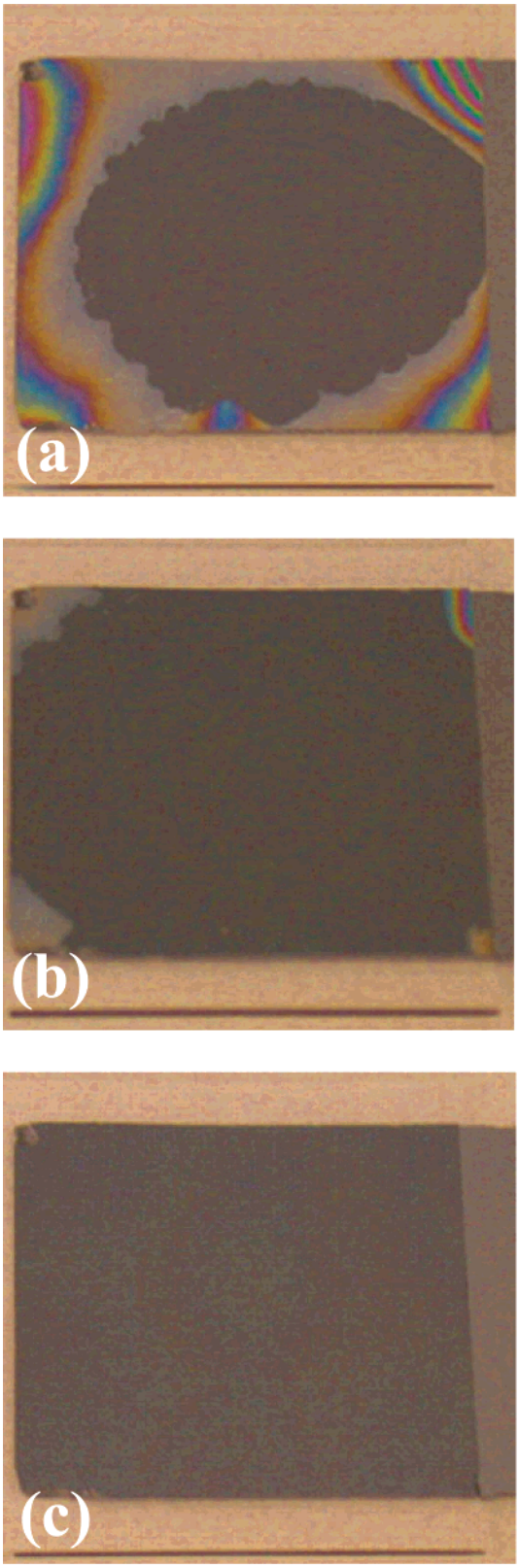

Figure 2. Still photos showing that trapped air is uniformly expelled by the liquid resist. Interference fringes spread out and disappear with time after contact between the mold and substrate: (a) 2 min; (b) 5 min; (c) 30 min.

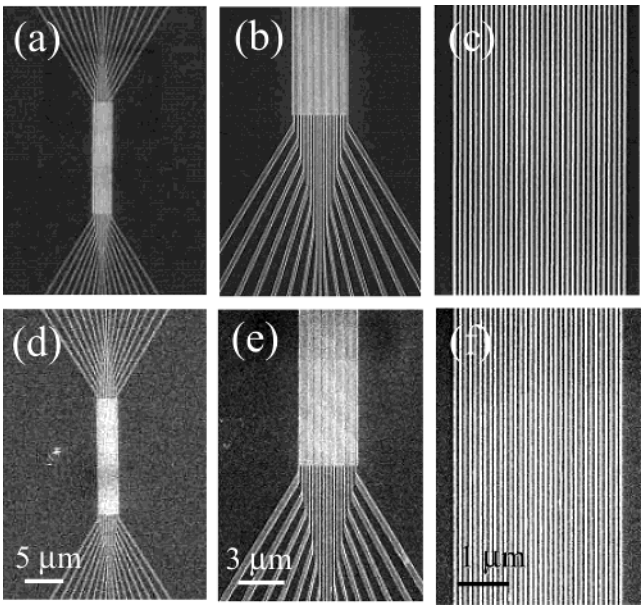

Figure 3. SEM images of 34 parallel nanowires with 100 nm pitch and their fan-out connections in the mold (a−c) and the corresponding metal bottom electrodes after lift-off (d−f).

E-beam evaporation was then used to deposit 4 nm Ti followed by 6 nm Pt onto the entire substrate with a rate of 0.5 nm/s at a pressure of 2×10^{-6} Torr. A final lift-off process to define the Ti/Pt bottom electrodes was performed with acetone in an ultrasonic bath to remove the cured resist and the metals above it. SEM images in Figures 3d−f show that the 34 parallel metal nanowires with 35 nm line width/50 nm half-pitch and their fan-out connections after lift-off were reproduced faithfully from the original relief structures in the mold. These images indicate that the UV-curable monomer liquid flowed well into the fine channels by capillary action during the mold−substrate contact period. The bottom electrodes remained over the entire imprinted area, confirming the uniformity of the imprinted resist and the lack of any residual layer.

The procedure for the deposition of the molecular monolayer of switching materials by the Langmuir−Blodgett (LB) method has already been reported previously.[7] After the LB film had been deposited, a Ti layer (7 nm) was evaporated onto it to protect it from damage during the deposition of the top electrode. In another investigation, we have shown that Ti reacts only at the top of the LB film and forms a protective layer against the subsequent Pt deposition.[9] Nanoimprinting for the top electrodes was performed on this Ti protective layer with the mold rotated 90 degrees to the bottom nanowires. A conventional mask aligner was used to align both the top and bottom images with a drop of liquid resist between the mold and the substrate. Platinum nanowires were patterned onto the substrate by repeating the same lift-off process for the bottom electrodes. Finally, to isolate each crosspoint electrically, the Ti layer was patterned with the Pt top electrode as a self-aligned mask by RIE with CF_4 and O_2 (4:1) gases at a pressure of 40 mTorr and a power of 200 W. Figure 4 shows the SEM images of one finished die with 34 × 34 crossed nanowires and the fan-out structure.

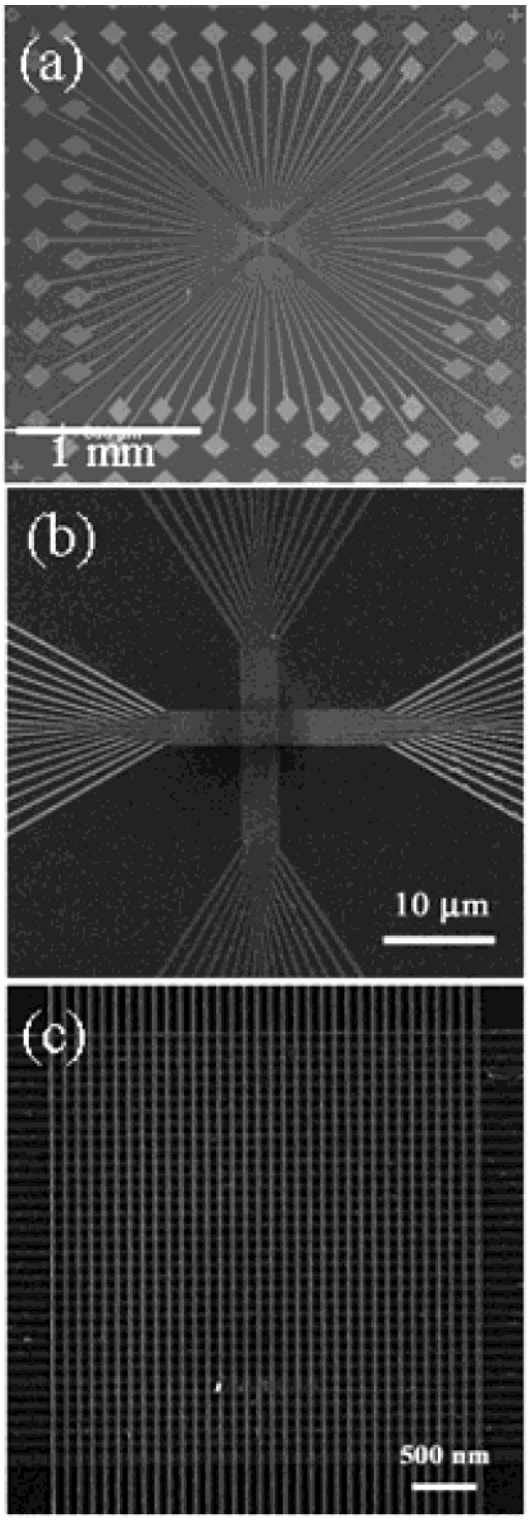

Figure 4. (a) SEM images of an array fabricated on the glass substrate; (b) the two perpendicular arrays of nanowires connected to micron-scale wires; (c) 34 × 34 nanowire crossbar structure.

The 34 top nanowires crossed over the 34 bottom nanowires with few visible defects. The cell density was equivalent to a bit density of 10 Gbit/cm^2. The electrical testing of this device array as a memory and logic integrated circuit is under investigation and will be reported separately.

We have developed a single-layer UV-nanoimprint liftoff process and demonstrated its utility by fabricating a 34 ×

34 crossbar with nanowires at a pitch of 100 nm. Our liquid resist formulation allowed us to minimize the resist layer thickness after curing without resorting to high imprint pressure. We also eliminated the problem of trapped air during contact by engineering the surface energy of the substrate such that it spread the resist and expel trapped air uniformly. Overall, our process required fewer processing steps than any bilayer process and yielded high-quality robust results at 50 nm half-pitch, which were confirmed by SEM.

References

(1) Chou, S. Y.; Krauss, P. R.; Renstrom, P. J. *Science* **1996**, *272*, 85.
(2) Chen, Y.; Jung, G. Y.; Ohlberg, D. D. A.; Li, X.; Stewart, D. R.; Jeppesen, J. O.; Nielsen, K. A.; Stoddart, J. F.; Williams, R. S. *Nanotechnology* **2003**, *14*, 462.
(3) Colburn, M.; Johnson, S.; Stewart, M.; Damle, S.; Bailey, T.; Choi, B.; Wedlake, M.; Michaelson, T.; Sreenivasan, S. V.; Ekerdt, J.; Willson, C. G. *Proc. SPIE* **1999**, *3676*, 379.
(4) Smith, B. J.; Stacey, N. A.; Donnelly, J. P.; Onsongo, D. M.; Bailey, T. C.; Mackay, C. J.; Sreenivasan, S. V.; Banerjee, S. K.; Ekerdt, J. G.; Willson, C. G. *Proc. SPIE* **2003**, *5037*, 1029.
(5) Perret, C.; Gourgon, C.; Micouin, G.; Grolier, J. P. *Jpn. J. Appl. Phys.* **2002**, *41*, 4203.
(6) Hiroshima, H.; Inoue, S.; Kasahara, N.; Taniguchi, J.; Miyamoto, I.; Komuro, M. *Jpn. J. Appl. Phys.* **2002**, *41*, 4173.
(7) Jung, G. Y.; Ganapathiappan, S.; Li, X.; Ohlberg, D. A. A.; Olynick, D. L.; Chen, Y.; Tong, W. M.; Williams, R. S. *Appl. Phys. A* **2004**, *78*, 1169.
(8) Chen, Y.; Ohlberg, D. A. A.; Li, X.; Stewart, D. R.; Williams, R. S. *Appl. Phys. Lett.* **2003**, *82*, 1620.
(9) Chang, S. C.; Li Z.; Lau, C. N.; Larade, B.; Williams, R. S. *Appl. Phys. Lett.* **2003**, *83*, 3198.

NL049487Q